

Plasmodium falciparum parasitaemia described by a new mathematical model

L. MOLINEAUX¹, H. H. DIEBNER^{2,3}, M. EICHNER², W. E. COLLINS⁴, G. M. JEFFERY⁵
and K. DIETZ^{2*}

¹World Health Organization (Retired)

²Department of Medical Biometry, University of Tübingen, Westbahnhofstrasse 55, D-72070 Tübingen, Germany

³Center for Art and Media, Lorenzstrasse 19, D-76135 Karlsruhe, Germany

⁴Centers for Disease Control and Prevention, US Public Health Service, Department of Health and Human Services, Atlanta, GA, USA

⁵U.S. Public Health Service (Retired)

(Received 27 April 2000; revised 13 October 2000; accepted 15 October 2000)

SUMMARY

A new mathematical model of *Plasmodium falciparum* asexual parasitaemia is formulated and fitted to 35 malaria therapy cases making a spontaneous recovery after primary inoculation. Observed and simulated case-histories are compared with respect to 9 descriptive statistics. The simulated courses of parasitaemia are more realistic than any previously published. The model uses a discrete time-step of 2 days. Its realistic behaviour was achieved by the following combination of features (i) intra-clonal antigenic variation, (ii) large variations of the variants' baseline growth rate, depending on both variant and case, (iii) innate autoregulation of the asexual parasite density, variable among cases, (iv) acquired variant-specific immunity and (v) acquired variant-transcending immunity, variable among cases. Aspects of the model's internal behaviour, concerning variant dynamics, as well as the respective contributions of the three control mechanisms (iii)–(v), are displayed. Some implications for pathogenesis and control are discussed.

Key words: *Plasmodium falciparum*, mathematical model, malaria therapy, PfEMP1.

INTRODUCTION

Plasmodium falciparum malaria is a major cause of morbidity and mortality, largely attributable to asexual parasitaemia. A realistic simulation model of the course of asexual parasitaemia in the human host is, therefore, relevant for the planning and evaluation of malaria control. We have recently reviewed published intra-host models of malaria, questioning the realism of their assumptions and behaviour, and suggesting a more rigorous comparison with data, the investigation of combinations of types of parasite diversity and density regulation mechanisms, allowance for individual variation, and the adoption of discrete-time modelling (Molineaux & Dietz, 1999). This paper presents a first implementation of those suggestions. It is based on 35 cases of primary *P. falciparum* infections inoculated for malaria therapy, and classified as spontaneous cures from malaria. We present (i) a statistical description of the data, proposed as a simulation target, (ii) a new simulation model of the course of *P. falciparum* asexual parasitaemia in the human host, (iii) a comparison of

model outputs with the simulation target and (iv) some aspects of the model's internal behaviour.

MATERIALS AND METHODS

The original data

Malaria therapy data have made a major contribution to our knowledge of patterns of asexual parasitaemia, for different species of human malaria parasites, including *P. falciparum*. The data used here were collected by the USPHS in the NIH Laboratories in Columbia, South Carolina and Milledgeville, Georgia, at a time when malaria therapy was a recommended treatment for neurosyphilis. The patients were Afro-American adult neurosyphilitics with no history of prior exposure to malaria. The parasite of choice for malaria therapy was *Plasmodium vivax*, to which Afro-Americans were, however, found to be refractory. So they were treated with different strains of *P. falciparum*, under close medical supervision. They were inoculated either with sporozoites (generally through mosquito bite) or with infected blood. Inoculations were preceded by variable sequences of blood and mosquito passages of the strain. Microscopical examination of the blood was performed on an almost daily basis. In principle 0.1 µl of blood was examined, less in the case of high density,

* Corresponding author: Department of Medical Biometry, University of Tübingen, Westbahnhofstrasse 55, D-72070, Tübingen, Germany. Tel: +49 7071 29 72112. Fax: +49 7071 29 5075. E-mail: klaus.dietz@uni-tuebingen.de

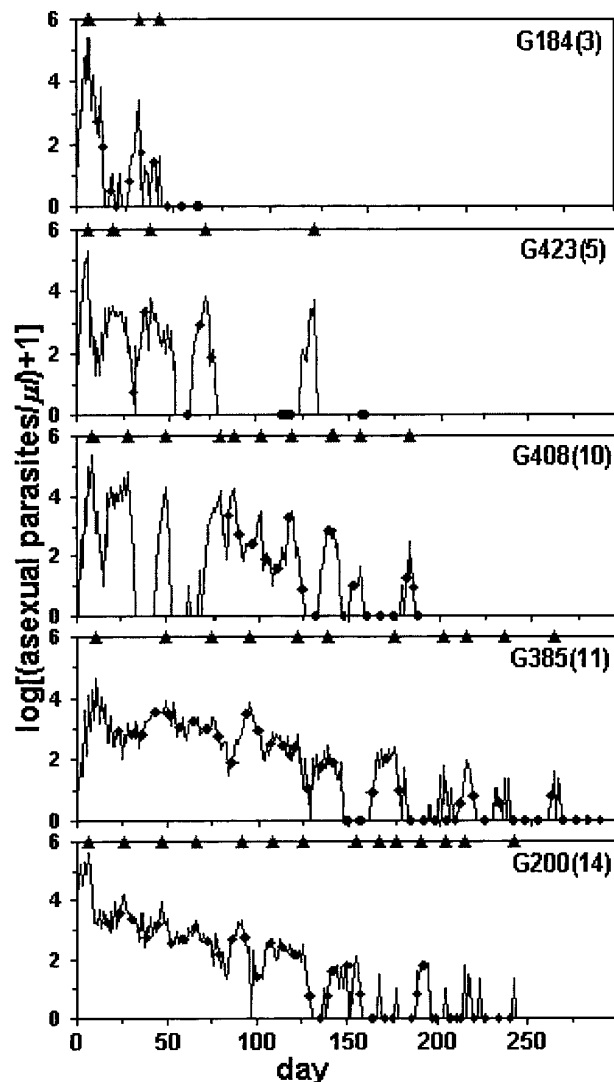


Fig. 1. Five observed case-histories of daily asexual parasitaemia. Selection: the 35 cases were ranked by increasing number of local maxima (the density on day t was declared a local maximum if it was higher than the densities on days $(t-6)$ to $(t-1)$ and not lower than on days $(t+1)$ to $(t+6)$); the cases ranked 1, 9, 18, 27, 35 were selected. The number of local maxima is given in parentheses, and their timing indicated by the triangles on top of each graph. Missing observations are substituted by log-linear interpolation, and the interpolated values identified by lozenges.

occasionally more; the detection threshold was thus about 10 parasitized red blood cells (PRBC) per μl (Earle & Perez, 1932; Eyles & Young, 1951; Jeffery & Eyles, 1954; Jeffery *et al.* 1959; Collins & Jeffery, 1999).

This investigation is restricted to 35 *P. falciparum* infections classified as spontaneous cures, out of a total of 334 primary inoculations. This classification was made as follows (i) a small fraction (19/334 or 5.7%) of the cases were terminated by an early curative treatment (most commonly a 3-day course of chloroquine), started within days 1 to 21, in the presence of fever and parasitaemia; they constitute a

non-random subset of relatively severe infections and were excluded from this investigation, (ii) most of the remainder were given a curative treatment at the end of their initial period of continuous or nearly continuous parasitaemia (i.e. after the period of expected effect on the neurosyphilis) and (iii) an apparently unselected subset of patients was recruited in an investigation of the total duration of infection in naive hosts (important at the time for the malaria eradication strategy) and not given their final curative treatment until they were continuously negative for 1 month of quasi daily blood examination, plus 5 months of twice weekly examination; they were then, as a rule, given a curative treatment before discharge, but classified as spontaneously cured; these patients are the subjects of the present investigation. About half of the cases belonging to categories (ii) and (iii) received, on the basis of their clinical and parasitological findings, 1 or more low-dose suppressive treatments (most commonly a single dose of quinine). Among the 35 cases of the present investigation, 16 received from 1 to 10 low-dose suppressive treatments (median 2; quinine was used 24 times, chlorguanide 21 times, chloroquine twice). These treatments had only a limited and short-lived effect on the course of parasitaemia and are not taken into account in the analyses presented. Eighteen patients were inoculated using infected blood, 17 by mosquito-bite; the *P. falciparum* strains inoculated were El Limon (Panama, 1948; 17 cases), Santee Cooper (South Carolina, 1946; 17 cases), and McLendon (South Carolina, 1940; 1 case).

Fig. 1 illustrates 5 contrasting observed case-histories. The raw data show much variation, of different kinds, both within and among individual case-histories. We try to develop a model with biologically plausible assumptions and parameter ranges, which produces a population of simulated case-histories that is statistically similar to the population of observed case-histories. Therefore, we need to reduce the raw data to a relatively short list of variables whose distributions can be used as quantified simulation targets. The following features are apparent on inspection of the data (i) a variable total duration of parasitaemia, including variable periods of non-patency (in these data, patent parasitaemia signifies a parasite density of ≥ 10 parasites/ μl), (ii) an initial period of increase, at a rapid and variable rate, up to a first local maximum, of variable height, (iii) a variable number of local maxima, at irregular intervals, (iv) an almost monotone downward trend of the local maxima, the first local maximum being usually the absolute maximum and (v) bouts of 2-day periodicity, in particular at high parasite densities.

The simulation targets

We opted not to take into account the 2-day

Table 1. The variables used to summarize a case-history of asexual parasitaemia (observed on odd days or simulated) and the results of paired *t*-tests (see Fig. 2)

| Variable | Code | Explanation | Mean (sim. – obs.) | <i>P</i> * |
|--|----------------|--|--------------------|------------|
| (1) Initial slope | init. slope | The slope of a linear regression line through the log densities from first positive slide to first local maximum | –0.0095 per day | 0.65 |
| (2) Log density at first local maximum | log 1st max. | The density at time <i>t</i> is declared a local maximum if it is higher than densities at times (<i>t</i> –6), (<i>t</i> –4), (<i>t</i> –2) and not lower than at times (<i>t</i> +2), (<i>t</i> +4), (<i>t</i> +6) | 0.037 | 0.082 |
| (3) Number of local maxima | No max. | | 0.51 | 0.41 |
| (4) Slope of local maxima | slope max. | The slope of a linear regression line through the log densities of the local maxima | –0.0035 per day | 0.0021 |
| (5) Geometric mean (GM) of the intervals between consecutive local maxima | GM interv. | | –3.7 days | 0.030 |
| (6) SD of the logs of the intervals between consecutive local maxima | SD log interv. | | 0.0003 | 0.99 |
| (7) Proportion of positive observations in the first half of the interval between first and last positive day | prop. + 1st | Day 1 = first positive day; ‘positive’ means density $\geq 10/\mu\text{l}$ | 0.115 | $<10^{-4}$ |
| (8) Proportion of positive observations in the second half of the interval between first and last positive day | prop. + 2nd | | 0.086 | 0.040 |
| (9) Last positive day | last + day | Difference between last and first positive day | 7 days | 0.64 |

* Before Bonferroni-Holm adjustment for the number of tests (see text)

periodicity. We wanted to explore to what extent we could simulate the course of asexual parasitaemia by a discrete-time model with 2-day steps. Accordingly we read the data on alternate days (even or odd), which had a smoothing effect. Table 1 lists and defines the 9 descriptive variables used to summarize a case-history, either observed or simulated. The 2 observed distributions (odd days, even days) were compared by the paired *t*-test: the only significant difference $P < 5\%$ was that the first local maximum was higher on odd than on even days; inspection of the data shows that this is probably related to the frequent association of the initial slope with a 2-day periodicity of the parasite density. Correlation coefficients were calculated for the $(9 \times 8)/2 = 36$ pairs of variables within each of the 2 observed distributions (not shown); the odd-day and even-day observations were strongly and positively correlated. We opted to compare our simulations with the odd day observations. The corresponding statistics are given in Table 2. They constitute our first simulation targets.

The model, its assumptions and their biological justifications

The model equations and the definitions of variables

and parameters are given in the Appendix. The model describes the time-course of asexual *P. falciparum* parasitaemia following a single monoclonal infection of an individual human host without previous exposure to malaria. It is a discrete-time model with 2-day steps, corresponding to the duration of *P.f.*'s erythrocytic cycle; time is expressed in days, parasitaemia as PRBC per μl . The population of PRBC is distributed among intraclonal variants of the main antigen (PfEMP1 = *P. falciparum* erythrocyte membrane protein 1) expressed on their surface. It has been suggested that the persistence of *P. falciparum* infections, at least in naive hosts, depends largely on intraclonal variation of antigen PfEMP1, displayed on the surface of PRBC's – a single variant being expressed per PRBC – and crucial for their sequestration (Borst *et al.* 1995). In *Plasmodium knowlesi* and *Plasmodium chabaudi* there is direct *in vivo* evidence of the association between successive recrudescences of parasitaemia and expression of different variants of those parasites' PfEMP1 analogues (Brown & Brown, 1965; Phillips *et al.* 1997). The initially estimated number of variants per *P.f.* genome was 50–150, but recent estimates are smaller, e.g. 41 in clone 3D7 (Sutherland, 1998). Our simulations

Table 2. Observed statistics (odd days)

| Variable* | Code | Minimum | Median | Maximum |
|-----------|----------------|----------------|----------------|-----------------|
| 1 | init. slope | 0.188 per day | 0.487 per day | 0.872 per day |
| 2 | log 1st max. | 3.37 | 4.79 | 5.66 |
| 3 | No max. | 2 | 10 | 17 |
| 4 | slope max. | -0.074 per day | -0.013 per day | -0.0007 per day |
| 5 | GM interv. | 14.4 days | 20.0 days | 77.8 days |
| 6 | SD log interv. | 0.03 | 0.20 | 0.47 |
| 7 | prop. + 1st | 0.40 | 0.88 | 1.00 |
| 8 | prop. + 2nd | 0.08 | 0.46 | 0.94 |
| 9 | last + day | 37 days | 215 days | 405 days |

* See Table 1.

assume 50 variants per clone, of which a variable number are expressed in the course of a case-history. The model dynamics (equation (1)) are driven by 2 forces: the switching among variants and the multiplication of a variant.

Switching dynamics among variants is expressed by $\left[(1-s)P_i(t) + sp_i(t)\sum_{j=1}^v P_j(t) \right]$ in equation (1), where $P_i(t)$ is the density of variant i , as PRBC/ μ l blood and $p_i(t)$ is the probability that a switching PRBC switches to variant i . A constant fraction (s) of PRBC switch variants per 2-day-cycle. Initially they switch into variant 1, 2, ..., v according to a geometric distribution with negligibly small probabilities of switching into the higher-numbered variants. Later, as variant-specific immune responses develop, switching into variants against which there is already a specific immune response is reduced accordingly (equation (4)), and the probabilities of switching into higher-numbered variants upgraded through normalising the sum of residual probabilities to 1. The model assumes that the host's variant-specific immune status affects variant expression in the course of intra-erythrocytic schizogony, thus reducing subsequent immunoselection.

These assumptions concerning switching dynamics are based on biological observations. In *P. falciparum* the switch-rate has been estimated only *in vitro* and the most commonly quoted estimate is 2% per cycle (Roberts *et al.* 1992). In *P. chabaudi* the switch-rate has been estimated *in vivo*, yielding minimum estimates of 1.2–1.6% per cycle (Brannan, Turner & Phillips, 1994). That variants can differ greatly in their intrinsic probability of expression has been shown directly in *P. chabaudi* in naive hosts (Brannan *et al.* 1994). Modulation of variant expression by the host's variant-specific immune status in the course of intra-erythrocytic schizogony is strongly suggested by findings in *P. knowlesi* (Brown, 1973; Barnwell *et al.* 1983).

Multiplication dynamics of a variant is expressed by $m_i S_c(t) S_i(t) S_m(t)$ in equation (1). A variant has a baseline multiplication factor (m_i), interpretable as the number of successful merozoites produced per PRBC in the absence of any controlling feedback, i.e.

in the very early stages of parasitaemia. For each simulation of a case-history, variant-specific baseline multiplication factors are randomly chosen from a truncated normal distribution. Among 4 *P. chabaudi* variants whose growth was compared *in vivo*, 1 showed a strong preference for reticulocytes and yielded a much lower maximum parasitaemia (Phillips *et al.* 1997). Our data show large variation of the initial slope of the parasitaemia, which led us to assume large variation of variant-specific growth rates, *plus* random host-specific association between a variant's growth rate and its intrinsic probability of expression, hence its probability of being expressed early in a case-history. The fact that in the *P. chabaudi*-mouse model, variation of growth rates among hosts was negligible in comparison with variation among variants, is not an objection, because human populations are genetically much more diverse than highly inbred laboratory mice.

Parasite multiplication is controlled by 3 independent (and competing) immune responses, 1 innate and variant-transcending, 1 acquired and variant-specific, 1 acquired and variant-transcending. The effects of the 3 immune responses are represented by the functions $S_c(t)$, $S_i(t)$ and $S_m(t)$. The existence and importance of an innate autoregulation of density is well established; it is a rapid and short-lived effect of the rupture of mature PRBC's via malaria toxin(s) and host cytokines (TNF, etc) and their secondary effectors (fever, NO) (Kwiatkowski, 1995). The wide variation in strength of that mechanism among hosts is suggested by the wide variation in density of the first local maximum in the malaria therapy data (Jeffery *et al.* 1959). The existence and importance of acquired variant-specific protective immunity are suggested by field observations (Bull *et al.* 1998). Most experts agree that acquired protective immunity against the asexual bloodstages has, in addition, some variant-transcending component(s). The immune response's effects are formulated as success probabilities (i.e. probabilities that the parasite escapes their effects), in terms of their triggers (parasite densities), without explicit modelling of their effectors (e.g. cytokines,

immune cells, antibodies). As the 3 immune responses are independent and competing, the probability that the parasite escapes the effects of all 3 is the product of the 3 success functions. All 3 success functions are of the general shape $S = (1 - \beta)\{1 + [f(X)/X^*]^{\kappa}\}^{-1} + \beta$, where X is the trigger; S is a sigmoid function, decreasing from 1 (for $f(X) = 0$) to β (as $f(X) \rightarrow \infty$), through $S = (1 + \beta)/2$ for $f(X) = X^*$, a critical constant; the slope of the sigmoid function at the inflection point increases with the power κ ; note that in this paper, β has been set to zero in the equations for $S_c(t)$ and $S_i(t)$, but not in the equation for $S_m(t)$, i.e. the innate and the acquired variant-specific immune responses are allowed to reach 100% efficacy in one infection, whereas the maximum allowed efficacy of the acquired variant-transcending immune response is $[100(1 - \beta)]\%$. For the innate immune response, all PRBC are triggers and targets; a given day's parasite density exerts innate autoregulation in the next 2-day-interval only (no delay, no memory); the critical constant P_c^* is case-specific and is assumed to be proportional to the first local maximum parasite-density of a case (equation (9)). For the acquired variant-specific and variant-transcending immune responses, the triggers and targets are, respectively, the corresponding variant-specific PRBC and the total PRBC; delays (δ_v, δ_m) are introduced to account for the fact that it takes some time for antigens to produce immune effectors, and discount factors (σ, ρ) are introduced to allow immunity to decay; a saturation level (C) for the acquisition of variant-transcending immunity is introduced to prevent it from growing too fast; the existence of a saturation level is at least biologically plausible; the critical constant P_v^* is common to all variants and hosts; the critical constant P_m^* is case-specific, as suggested by the large variation in total duration of patent parasitaemia, and is assumed to be proportional to the total duration of a case (equation (10)).

Initial conditions and extinction rules are as follows. The initial parasitaemia is constituted by variant 1 and the initial density is set at $0.1/\mu\text{l}$, corresponding to 5×10^5 PRBC in an adult with a 5 l blood-volume, or to a density 100 times smaller than the detection level of $10/\mu\text{l}$. A variant goes extinct when its density drops below $10^{-5}/\mu\text{l}$, i.e. when its number drops below 50 in a adult blood volume of 5 l (it may reappear through switching from other variants); the infection goes extinct when all expressed variants have gone extinct.

Method of fitting

We did not apply formal minimization but used informed trial and error. Certain parameters were fixed, e.g. the mean 2-day baseline multiplication factor ($\mu_m = 16$) or the 2-day switching fraction ($s = 0.02$). Other parameters were varied, within ranges

based on the literature or on the raw data. Simulations were conducted in 2 phases. In the *first phase*, we performed sets of 35 simulations corresponding to the 35 observed case-histories. Between sets, 1 or more parameters were varied. Within each set, the parameters P_c^* and P_m^* and the random allocation of variant-specific baseline multiplication factors were case-specific. Simulation outcomes were compared to simulation targets (Table 2) by inspection, and a 'best' set was selected. In the *second phase*, starting from that best set, we simulated each case 50 times, reallocating randomly each time the variant-specific baseline multiplication factors, and used χ^2 to identify a 'best' case-specific matching between the variants' probability of expression and multiplication factor.

RESULTS

Fitting the model to the data

Simulations were conducted in 2 phases. In the first phase, we took, for each population of 35 case-histories, the following steps (i) specify initial conditions and parameter values for that population; after preliminary exploration, the initial conditions were set at $P_i(0) = 0.1$ for $i = 1$, and $P_i(0) = 0$, for $i = 2, 3, \dots, v$; use the parameters k_c and k_m to calculate host-specific values of P_c^* and P_m^* , (ii) for each simulation: randomly select variant-specific values of m_i and conduct the simulation to extinction, (iii) add the effect of measurement error, assuming a Poisson distribution for the number of PRBC per $0.1 \mu\text{l}$: for expected values less than 100 replace the simulated result by a Poisson distributed random number with the corresponding expectation; for expected values above 100 sample a Poisson random variable with mean 100 and multiply it with the appropriate correction factor; this method assumes that for high densities of PRBC only about 100 cells are actually counted, (iv) after completion of the simulated case-histories, summarize them by the same statistics as used to summarize the observed case-histories, and compare simulations to observations, in terms of minimum, median, maximum of the 9 descriptive variables (see Table 2). Except for the stochastic steps (ii) and (iii), the simulations are deterministic. The parameter values that produced the 'best' population of simulated case-histories are given with the list of parameters in the Appendix.

In the second phase of simulations, for each host-specific pair of P_c^* and P_m^* , 50 simulations were conducted, each with a new allocation of m_i values to variants, while leaving the other parameters unchanged. Within each set of 50 simulations, the fit between each simulation and the corresponding case-history (i.e. the case used to calculate the case-specific P_c^* and P_m^* inputs) was measured by a χ^2 statistic which gave equal weight to the normalized

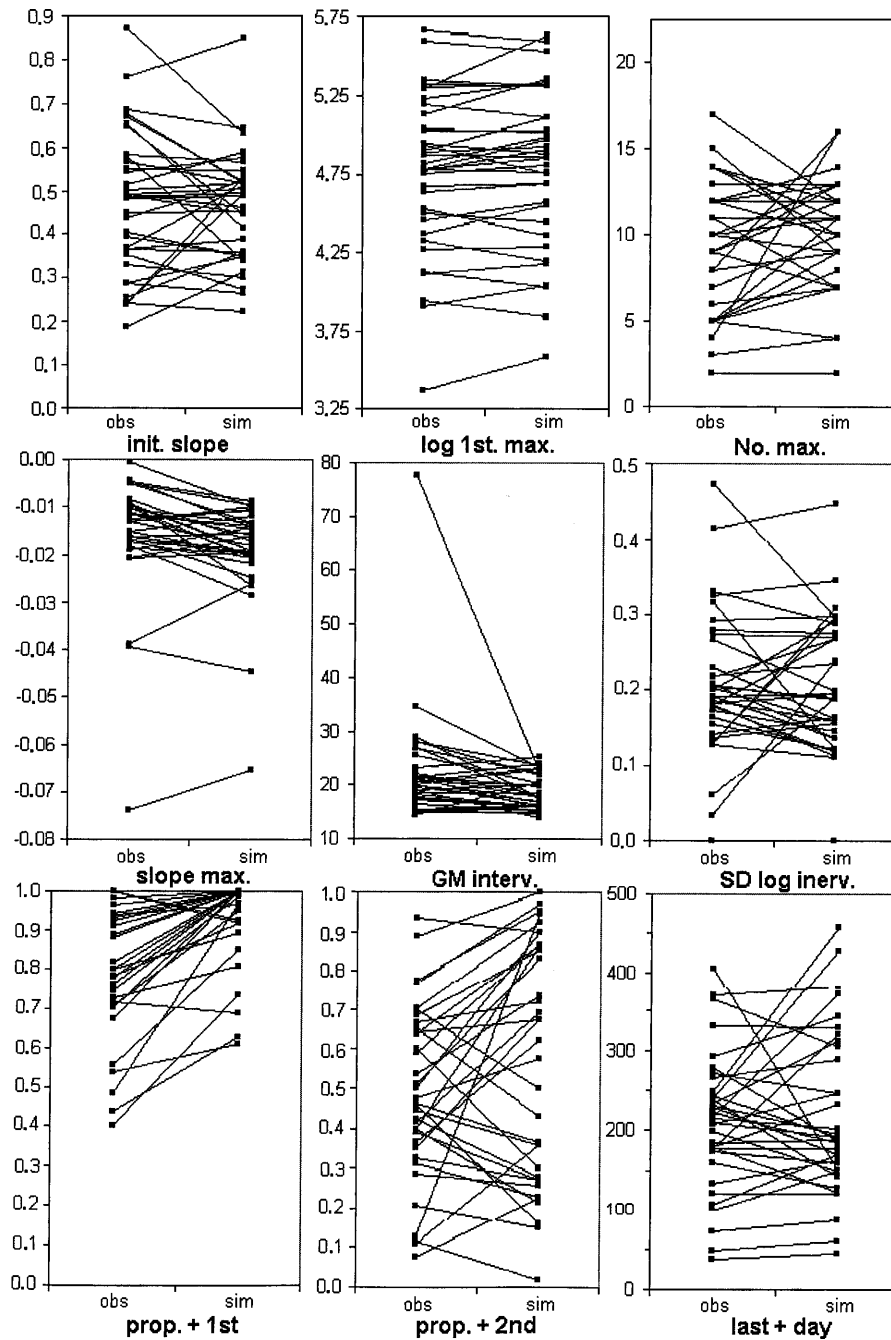


Fig. 2. Paired t -test comparisons of 35 simulated case-histories with the corresponding odd-day observed case-histories, with respect to the 9 descriptive variables. Each simulated case-history is the best (by least χ^2) out of 50 stochastic realizations. Variables, mean differences (between observed and simulated) and P values are given in Table 1.

residuals of the 9 descriptive variables. The simulation with the least χ^2 was designated best. The 35 best simulations were compared to the 35 observed case-histories by the paired t -test, and the results are shown in Fig. 2 and Table 1 (the table gives, for each variable, the mean difference between simulated and observed, and the P -value unadjusted for the number of tests). For all of the 9 variables the ranges of observed and simulated values are largely overlapping. After correction by the Bonferroni-Holm procedure for the number of comparisons made, the model outputs differ significantly ($P < 0.05$) from the observations with respect to 2 of the 9 variables (i)

the simulated slope of local maxima (slope max.) is too steep, and (ii) the proportion of positive observations in the first half of the interval between first and last positive day (prop. + 1st) is too large. Note that for those two variables, most differences between observed and simulated are relatively small, but systematic, hence the low P values in the paired t -test. We also compared the Spearman rank correlation coefficients between pairs of descriptive variables of the simulations with those of the observations, as shown in Fig. 3; the agreement between observed and simulated correlations is remarkably good.

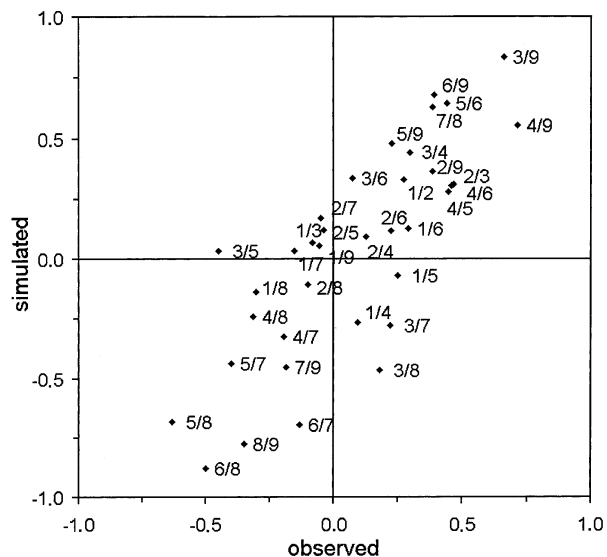


Fig. 3. Spearman's rank correlation coefficients between pairs of descriptive variables (numbered 1–9 as in Table 1) in the 35 best simulated case-histories and in the 35 observed case-histories.

To illustrate the variability within the sets of 50 simulations, and to show some 'best fits', we selected the 1st, 3rd and 5th case of Fig. 1, representing a wide range of numbers of local maxima. Fig. 4 shows the distribution of the 3 sets of 50 simulations, with respect to 3 of the 9 descriptive output statistics (init. slope, No. max., slope max.); for each distribution, the corresponding observation is added, and the 'best' simulation identified. The stochastic allocation of growth factor (m_i) to variants produces a large variation in the outputs; the observed values lie within the range of the 50 simulations in 7 of the 9 distributions shown, and just outside in the remaining 2. The best runs, within each of the 3 sets of 50, are shown in Fig. 5, in comparison with the corresponding observations. The simulated case-histories are rather similar to the corresponding observed case-histories.

The model's internal behaviour

It should be of interest to modellers and biologists to find out how the model's internal behaviour generates the rather realistic patterns of asexual parasitaemia obtained. This section and Figs 6–8 make explicit some aspects of that internal behaviour. The features displayed cannot be tested with malaria therapy data, but might be tested with data from other sources.

Fig. 6 illustrates the variants' behaviour according to the model; it shows, for the best run of case G408, the total density plus the density of 10 selected variants out of the 50 expressed in that run. Low-numbered variants are expressed early because of a high $p_i(0)$ (equation (4)), and compete through their growth factors. At the first local maximum ($P_c(14) \approx$

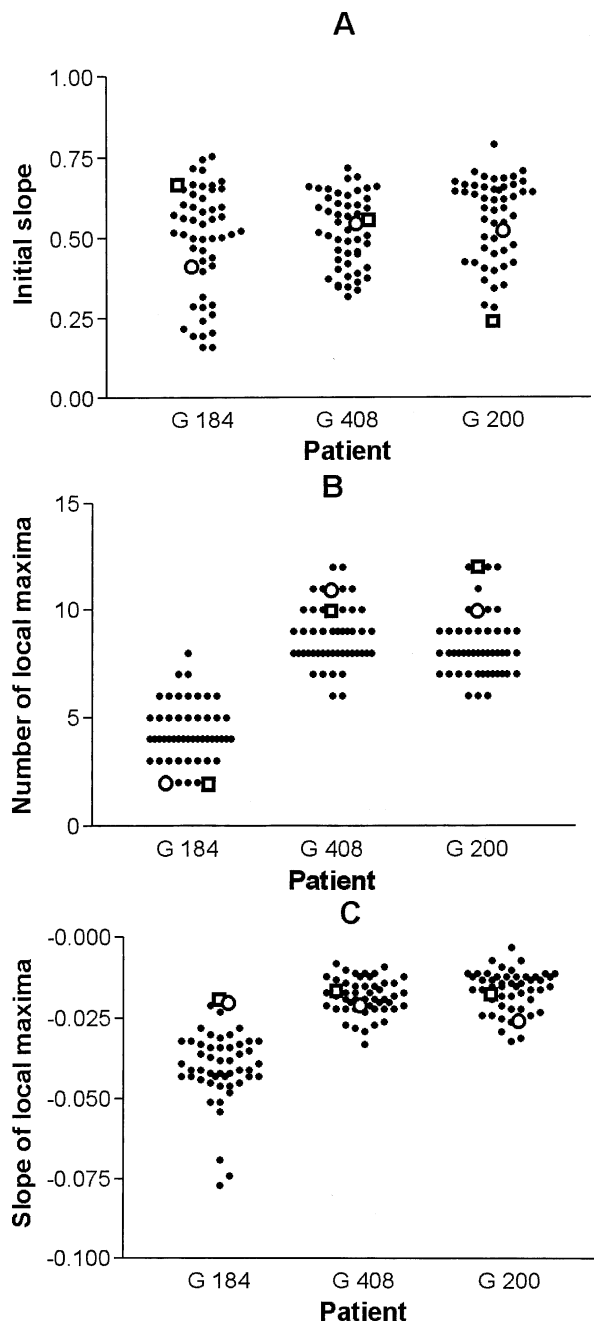


Fig. 4. Distributions of 3 of the 9 descriptive variables: (A) initial slope; (B) number of local maxima; (C) slope of local maxima in 3 sets of 50 simulations, corresponding to the 1st, 3rd and 5th case of Fig. 1, representing a wide range of numbers of local maxima. The P_c^* and P_m^* parameters are case-specific and fixed for the 50 runs of the case; for each run within each set of 50, the parameter m_i is randomly allocated to the variants, from the distribution given in Table 2. For each distribution, the corresponding observation is added (□) and the best simulation (by least χ^2) identified (○).

207000/ μ l): (i) 13 variants are expressed, 5 of them at $> 10/\mu$ l; (ii) variant 3, a fast grower ($m_3 = 30$) has overgrown variants 1 ($m_1 = 1.3$) and 2 ($m_2 = 12$), and makes up 91 % of the total; (iii) the innate success function reaches its lowest value in this run ($S_c(14)$

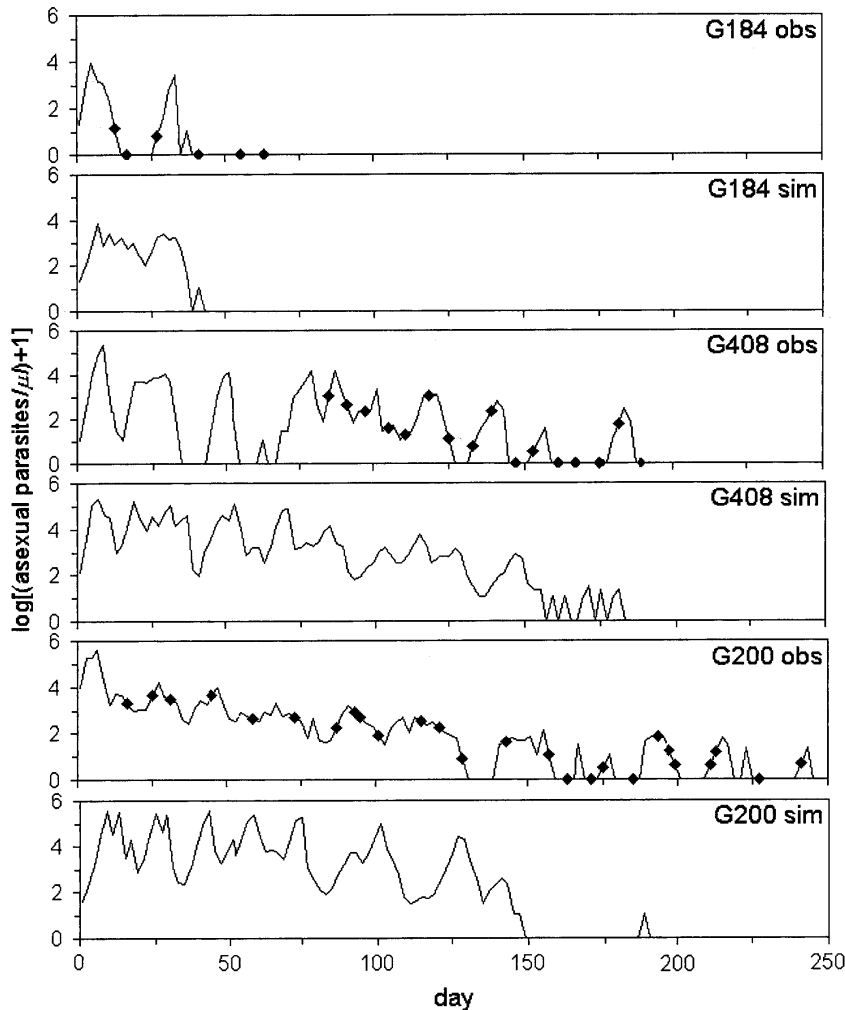


Fig. 5. Three contrasting observed case-histories (odd days) and the best (by least χ^2) out of 50 stochastic realisations of the corresponding simulations.

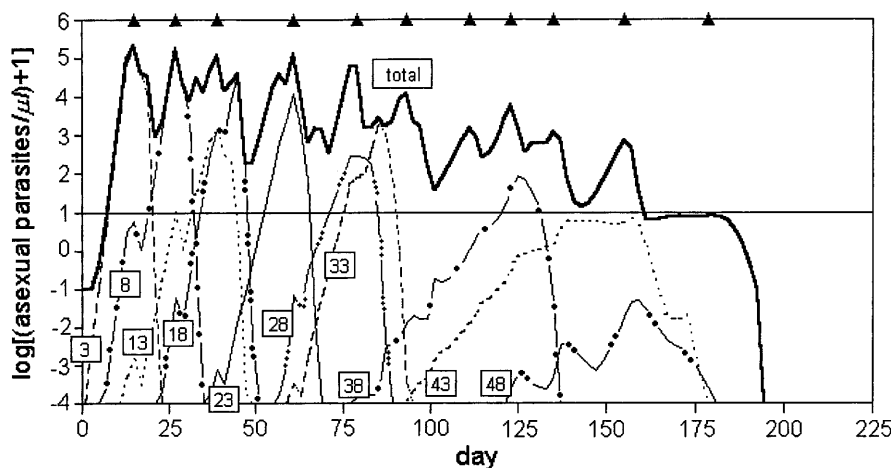


Fig. 6. Total and selected variant-specific asexual parasite densities in the best simulation of case G408; 50 variants were expressed, of which 10 (equally spaced) are shown, including those dominating the 1st and 2nd local maximum. Simulation starts on day zero with variant 1 at density $10^{-1}/\mu\text{l}$; local maxima are marked by triangles on top; the horizontal line indicates the microscopic detection level ($10/\mu\text{l}$); the simulation results shown precede the application, to the total, of a stochastic measurement error (see text), which, in this run, generated an 11th visible peak on day 178. The variants shown had the following stochastically allocated multiplication factors (rounded to the nearest integer):

| | | | | | | | | | | |
|---------|----|----|----|----|----|----|----|----|----|----|
| variant | 3 | 8 | 13 | 18 | 23 | 28 | 33 | 38 | 43 | 48 |
| m_1 | 30 | 23 | 14 | 33 | 23 | 15 | 27 | 5 | 9 | 5 |

= 0.01) and all variants drop (equation (1)). After the drop, variant 3 and 3 others (not shown) go on to extinction through variant-specific immunity (equation (7)), while most variants recover. High-numbered variants can appear only after the host's variant-specific immunity has raised their selection probability $p_i(t)$, while lowering the $p_i(t)$ of lower numbered variants (equation (5)). Among the 11 peaks of this run (8 in the first 125 days), the number of variants expressed varied from 3 (peak no. 11) to 15 (peak no. 4), and the contribution of the dominant variant varied from 69% (peak no. 3) to 99% (peak no. 10). Later peaks tend to be lower, with lower innate immunity and higher variant-transcending immunity, and to be composed of fewer variants, with a stronger dominance of the dominant variant. For example, at peak no. 8, on day 122, $P_c = 5769$; $S_c = 1.00$; $S_m = 0.13$; 9 variants are expressed, 4 of them at $> 10/\mu\text{l}$; the dominant variant makes up 95% of the total. Overall, the effects of differential variant-specific baseline expression probabilities ($p_i(0)$) and multiplication factors (m_i), of immunomodulation of expression probabilities, and of competition through innate density regulation, are strong.

Among the best runs of the 35 cases, the number of variants expressed varied from 12 to 50 (median 45); the number expressed at $> 10/\mu\text{l}$ varied from 8 to 50 (median 42); the two numbers were strongly correlated, and their ratio (i.e. the fraction of expressed variants reaching $> 10/\mu\text{l}$) varied from 0.53 to 1. The number of variants expressed at $> 10/\mu\text{l}$ was positively correlated with P_m^* (Spearman's $R = +0.70$; $P = 0.0001$), with the number of local maxima ($R = +0.58$; $P = 0.0003$), and with time from first to last patent parasitaemia ($R = +0.47$; $P = 0.004$). By linear regression we found that the number of local maxima increased with the number of variants expressed at $> 10/\mu\text{l}$, at the rate of 1 local maximum per 6 variants (in Fig. 6 the first wave of parasitaemia 'consumed' 4 variants).

Fig. 7 shows the relative contributions of the model's 3 control mechanisms in the 35 simulated cases, cumulated either over the whole case-history or only from onset to 6 days after the first local maximum. The calculation assumes the following (i) in the absence of control, the parasite population would grow according to $P_c(t+2) = \sum_{i=1}^v P_i(t)m_i$; (ii) the difference between that hypothetical $P_c(t+2)$ and the one calculated according to equations (1)–(3) represents the number of parasites 'controlled' in the interval $(t, t+2)$; (iii) the 3 control mechanisms compete to control variant i according to $(1 - S_k(t)) / [(1 - S_c(t)) + (1 - S_m(t)) + (1 - S_i(t))]$, where $k = c, m, i$; (iv) summation over a period of time gives – within that period – each controlled parasite an equal weight. Over the whole case-history, the innate variant-transcending immune response contributed

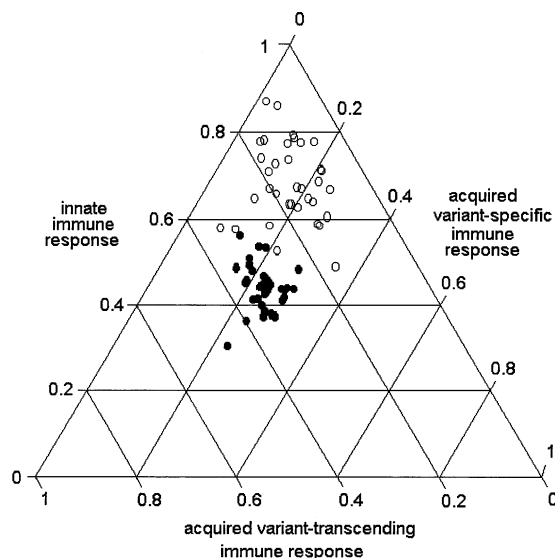


Fig. 7. Ternary plot of the relative contributions of the model's 3 control mechanisms in the 35 simulated cases, cumulated either over the whole case-history (●) or only from onset to 6 days after the first local maximum (○). The contributions are calculated as outlined in the text.

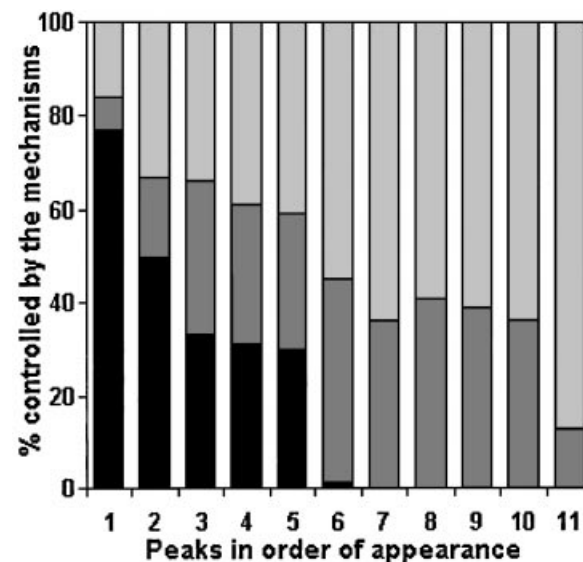


Fig. 8. The relative contributions of the model's 3 control mechanisms (■, innate immune response; ▒, acquired variant-specific immune responses; □, acquired variant-transcending immune response) in the control of the 11 successive peaks of parasitaemia of the best simulation of case G408. Each peak is identified by having a parasite density higher than the 3 preceding values, and not lower than the 3 following values. The contributions are calculated as outlined in the text, including for each peak the 4 intervals from $(t-4)$ to $(t+4)$, where $t =$ time of peak.

31–56% (median 44) of the total control, the acquired variant-specific immune responses 13–29% (median 23), and the acquired variant-transcending immune response 24–46% (median 33). For the

control of the early parasitaemia, up to 6 days after the first local maximum, the relative contributions of the 3 control mechanisms were quite different; the innate immune response contributed 49–87% (median 67) of the control, the acquired variant-specific immune responses 2–35% (median 16), and the acquired variant-transcending immune response 6–34% (median 15). Over the whole case-history the relative contribution of the innate density regulation is weakly negatively correlated with $\log P_c^*$ ($r = -0.18$; $P = 0.29$); the relative contribution of variant-transcending immunity is negatively correlated with P_m^* ($r = -0.62$; $P = 0.0001$). The relative contribution of the innate immune response to the control of early parasitaemia is weakly negatively correlated with $\log P_c^*$ ($r = -0.26$; $P = 0.14$).

Fig. 8 shows the relative contributions of the 3 mechanisms to control the successive peaks of parasitaemia of the best simulation of cases G408. According to the model, the innate immune response dominates during early control, and becomes progressively less important thereafter, while the acquired variant-transcending immune response, relatively unimportant for early control, becomes dominant in the later stages of the infection.

DISCUSSION

The work presented here is part of a larger project aiming at the development of malaria (*P. falciparum*) models more reliable than existing models for the planning and evaluation of intervention trials and control programmes, as well as for the discussion of strategic options concerning the development of new tools for malaria control. The course of asexual *P. falciparum* parasitaemia in the individual human host is a major node in the web of causation leading to morbidity and mortality. Modelling that course following a single inoculation in a non-immune individual is an appropriate first step, for which the daily follow-up of cases undergoing malaria therapy – when the latter was a recommended treatment for neurosyphilis – provide uniquely valuable data.

While the malaria therapy data are indeed uniquely valuable, some constraints, related either to their very nature or to the use made of them, should be kept in mind. (1) The patients are (neurosyphilitic) adults, while in endemic areas the most important group for the natural history of malaria are (non-syphilitic) children. (2) As our purpose was to simulate the natural history of *P. falciparum* intra-host parasitaemia, we limited ourselves to cases that could be classified as spontaneous cures, thus excluding the small minority of more severe cases that were, on clinical and/or parasitological grounds, given early curative treatment. (3) Two modes of infection (blood, sporozoites), and different parasite strains were used; the strains used (2 from the US,

1 from Central America) represent a very small non-random subset of existing *P. falciparum* populations; among the 35 cases classified as spontaneous cures, the subsets according to strain and mode of infection are too small to allow an adequate stratified analysis. However, study of the total number of primary *P. falciparum* infections convinced us that any differences among the 3 strains concerned, or between the 2 modes of infection were negligible in comparison with differences among cases. (4) We simulated the infections as if they were monoclonal, with a single pool of 50 variants; the actual mono- or polyclonality of the infections is unknown, although the repeated artificial passages, in particular through blood, may have driven the strains used towards monoclonality. To our knowledge the strains used have not been preserved, nor has any attempt been made to assess possible clonal diversity from preserved blood slides.

A review of published intra-host models of malarial asexual parasitaemia left us rather dissatisfied with their lack of realism (Molineaux & Dietz, 1999). We have the same reservation about the new model of Hoshen *et al.* (2000). It is probably fair to claim that, in comparison with those models (leaving out those specifically designed to simulate the 2-day periodicity of asexual parasitaemia) the work presented here (i) sets more precise data-based simulation targets, (ii) compares simulations and observations more rigorously and (iii) produces more realistic patterns of asexual parasitaemia. It is important to consider whether the latter was achieved with biologically plausible assumptions and internal operations of the model.

With respect to the model's assumptions, extensive simulation (of which only the more conclusive part is shown), leads us to conjecture, albeit only through trial and error and incomplete sensitivity analysis, that the 5 following factors or *equivalents*, are necessary to achieve the level of realism actually obtained. (i) Intra-clonal antigenic variation, (ii) large variation of the variants' baseline growth rate, depending on both variant *and* case, (iii) innate autoregulation of the asexual parasite density, variable among cases, (iv) acquired variant-specific immunity and (v) acquired variant-transcending immunity, variable among cases.

We interpret the case-specific variation of factors (ii), (iii) and (v) as host-specific (genetically determined) variation in (a) growth rate of a given variant (perhaps related to variation in quality, quantity or distribution of cytoadherence receptors); (b) strength of the innate autoregulation of density, (related to variation in the cytokine response to a given amount of malaria toxin) and (c) efficacy of variant-transcending immunity, related to variation in immunosensitivity to variant-transcending antigens. We are currently analysing multiple inoculations in the malaria therapy data to test the host-

specificity of variation in the innate and acquired variant-transcending control mechanisms. None of the published *intra-host* malaria models has the above combination of 5 factors; a trypanosomiasis model (Agur & Mehr, 1997) has the 5 factors, without mention of case-specific variation of any of them; on the other hand, in contrast to most *intra-host* malaria models, the model presented here does not model explicitly uninfected RBC, merozoites, or immune effectors (Molineaux & Dietz, 1999).

Biological justifications for the model's assumptions have been presented above. They are, admittedly, not compelling, and our simplifying assumptions should be critically reviewed. With respect to antigenic variants, the main difficulty encountered was to balance consumption and spacing by means of biologically plausible mechanisms. Consumption is achieved through variant-specific immunity with a steep success function (equation (7), $\kappa_v = 3$). The following assumptions contribute to spacing. (i) A baseline probability of expression following a geometric probability law (equation (4)), sufficiently steep ($q = 0.3$) to ensure that, initially, many variants have a negligibly low probability of expression. (ii) Strong modulation of the probability of expression by the host's variant-specific immune status (equation (5)). (iii) Wide variation of the variants' baseline multiplication factors, independently of their baseline probability of expression (the main stochastic element of the simulations; it can have a large effect). (iv) Competition through innate autoregulation of density (early in the infection).

What kind of – biologically plausible – mechanism of variant expression is likely to be selected by evolution? Intraspecific evolution of *P. falciparum* is likely to take place mainly in areas of intense transmission, because of large mutation denominators, high rates of genetic recombination in the vector, and intense selection pressure from human immune responses. In such areas, *P. falciparum* is inoculated into human hosts with very diverse repertoires of variant-specific immunities. If (i) PfEMP1 is crucial for sequestration, (ii) successful sequestration is crucial for the parasite's growth and (iii) variant-specific immunity prevents successful sequestration, then the parasite's fitness would be increased by a mechanism allowing the parasite, on entering a new host's blood-stream, to explore its own variant repertoire fast enough to find rapidly some variant(s) likely to be successful in that host at that time (i.e. with a sufficient baseline growth rate, and not too strongly affected by the host's repertoire of variant-specific immunities), while saving some variants for long enough to adapt the period of potential gametocytogenesis (out of asexual parasites) to the time-dependent vectorial capacity (e.g. to bridge more or less extensive periods in which vectorial capacity is very low or zero). Such a

mechanism is assumed in the model proposed here, but nature's solution may be quite different, and we are currently comparing alternative models of variant expression, in terms of assumptions, inputs, internal behaviour, outputs and measures of fit to data.

One of the more problematic assumptions of the model presented is the strong case dependence of the basic multiplication factor of a given variant, identified (numbered) by its baseline probability of expression. This case-dependence is such that the same variant may be the fastest growing – out of 50 – in one simulation, and the slowest growing in another. This allowed realistic simulation of the wide variation, among cases, of the initial slope of the parasite density, but may biologically be questionable. Also crucial in our simulations are the case-specificity of the strengths of innate density regulation and of variant-transcending acquired immunity and the estimation of the corresponding parameters (P_c^* , P_m^*) from related case-specific observations (the parasite density at its first local maximum and the total duration of parasitaemia, respectively). Our modelling of variant-transcending acquired immunity is admittedly a crude caricature, lumping its presumably multiple components into a single dimension. The model's assumptions and internal behaviour (e.g. concerning variant-dynamics and relative contributions of different mechanisms of density regulation), not testable with the data used, are likely to be challenged by the rather rapidly expanding knowledge of the biology of *P. falciparum*.

Implications about pathogenesis and control can only be speculative and conditional. If the model captures correctly the main features of *P. falciparum* infection, a major determinant of severe disease and death may be the inability to control the first local maximum of the asexual parasite density, and that inability may largely be due to the weakness of the innate cytokine response (TNF etc) to malaria toxin. The role of the cytokine response (TNF etc) involves an apparent paradox: on the one hand, a high TNF production per parasite should keep the parasite density down. On the other hand according to clinical observations, severity of disease, parasite density, and TNF concentration are positively correlated with each other (Grau *et al.* 1989; Kwiatkowski *et al.* 1990; Kremsner *et al.* 1995). This would imply a negative correlation between production of TNF per parasite and production (hence concentration) of TNF per host. A negative correlation was indeed observed between patients' TNF concentration and their white blood cells' TNF production *in vitro* in response to PHA (phytohaemagglutinin, used as a proxy for malaria toxin) (Kremsner *et al.* 1995). Weakness of the innate cytokine response to toxin could explain why only a minority of the exposed develop severe malaria, but could not, however, explain why some of them do so

after successfully controlling several or even many prior inoculations. That observation could be explained by a parasite factor (intrinsic virulence) and/or by a host–parasite mismatch (Molineaux, 1996), and either of these explanations might be applied to differences among clones or among variants within a clone. If innate density regulation is as important for the early control of acute malaria in non-immunes, as suggested by the simulations presented, then a purely anti-toxic vaccine may indeed be a two-edged sword, as conjectured by its opponents and as suggested – indirectly – by the results of 2 anti-TNF antibody trials (Kwiatkowski *et al.* 1993; Boele van Hensbroek *et al.* 1996).

Whether a given gain in model realism balances the corresponding cost in model complexity is not easy to decide. We conjecture that, for the foreseeable future, control measures, including vaccination, will not eradicate *P. falciparum* but modify the host–parasite balance, at the individual and population levels. If so, a simulation model, in order to be useful, should probably be rather realistic biologically. The work presented here may be a useful step in that direction, with respect to a crucial part of the parasite's life-cycle. We are currently working on a systematic sensitivity analysis of this model, including alternative or simpler assumptions, detection and understanding of the model's weaker points, and exploration of the implications for pathogenesis and control.

Support by the European Commission is acknowledged (Project No. IC 18-CT97-0242(DG 12-SNRD)). We thank the participants of the Concerted Action 'Mathematical models of the immunological and clinical epidemiology of *P. falciparum* malaria' for helpful discussions. We also thank Adrian Luty for his help with improving our English.

APPENDIX

The model's equations, variables, and parameters

The model is a discrete-time model, with step-size of 2 days; times are in days, concentrations per μl .

Equations

$$P_i(t+2)' = \left[(1-s)P_i(t) + sp_i(t) \sum_{j=1}^v P_j(t) \right] \times m_i S_c(t) S_i(t) S_m(t), \quad (1)$$

$$P_i(t+2) = \begin{cases} P_i(t+2)' & \text{if } P_i(t+2)' \geq 10^{-5}, \\ 0 & \text{otherwise} \end{cases}, \quad (2)$$

$$P_c(t) = \sum_{i=1}^v P_i(t), \quad (3)$$

$$p_i(t) = \begin{cases} 0 & \text{if } S_i(t) < 0.1 \\ \frac{q^i S_i(t)}{\sum_{j=1}^v q^j S_j(t)} & \text{otherwise,} \end{cases} \quad (4)$$

$$S_c(t) = \left(1 + \left(\frac{1}{P_c^*} P_c(t) \right)^{k_c} \right)^{-1}, \quad (5)$$

$$S_i(t) = \left(1 + \left(\frac{1}{P_v^*} \sum_{\tau=0}^{t-\delta_v} P_i(\tau) e^{-\sigma(t-\tau-\delta_v)} \right)^{\kappa_v} \right)^{-1}, \quad (6)$$

$$S_m(t) = (1-\beta) \left(1 + \left(\frac{1}{P_m^*} \sum_{\tau=0}^{t-\delta_m} \hat{P}_c(\tau) e^{-\rho(t-\tau-\delta_m)} \right)^{\kappa_m} \right)^{-1} + \beta, \quad (7)$$

$$\hat{P}_c(t) = \begin{cases} P_c(t), & \text{if } P_c(t) < C, \\ C & \text{otherwise} \end{cases} \quad (8)$$

$$P_c^* = k_c \times (\text{first local max. density}) \quad (9)$$

$$P_m^* = k_m \times [(\text{last pos. day}) - (\text{first pos. day})] \quad (10)$$

$$m_i \sim N(\mu_m, \sigma_m^2) \text{ truncated to ensure } m_i \geq 1, \quad (11)$$

Variables

| | |
|--------------------------|--|
| $P_i(t)$ | = density of variant i , as PRBC/ μl blood |
| $P_c(t)$ | = total parasite density, as PRBC/ μl blood |
| $p_i(t)$ | = probability that a switching PRBC switches to variant i |
| $S_c(t), S_i(t), S_m(t)$ | = probability that a parasite of variant i escapes control by the innate IR (IR = immune response), acquired variant-specific IR, and acquired variant-transcending IR, respectively, in the interval $(t, t+2)$ |

Parameters

| | | |
|--------------------------------|--|--|
| v | = number of variants per clone | [parameter values used in the simulations] [$v = 50$] |
| s | = fraction of parasites switching among variants per two-day cycle | [$s = 0.02$] |
| q | = parameter of the geometric distribution of switching probabilities | [$q = 0.3$] |
| m_i | = basic multiplication factor, per two-day cycle, of variant i ; $m_i \sim N(\mu_m, \sigma_m^2/m_i \geq 1)$ | [$\mu_m = 16$; $\sigma_m = 10.4$] |
| P_c^*, P_m^* | = two host-specific critical densities | |
| k_c, k_m | = two constants allowing calculation of P_c^*, P_m^* from host-specific data | [$k_c = 0.2$; $k_m = 0.04$] |
| P_v^* | = critical density of a variant, common to all variants | [$P_v^* = 30$] |
| $\kappa_c, \kappa_v, \kappa_m$ | = stiffness parameters for saturation of innate IR, acquired variant-specific IR, and acquired variant-transcending IR, respectively | [$\kappa_c = 3$, $\kappa_v = 3$, $\kappa_m = 1$] |
| C | = maximum daily antigenic stimulus, per μl , of the acquired variant-transcending IR | [$C = 1$] |

| | | |
|----------------------|---|-----------------------------|
| σ, ρ | = decay parameters, per day, of the acquired variant-specific and variant-transcending IR's, respectively | $[\sigma = 0.02; \rho = 0]$ |
| δ_v, δ_m | = delay parameters, in days, of the acquired variant-specific and variant-transcending IR's, respectively | $[\delta_v = \delta_m = 8]$ |
| β | = minimum value of S_m | $[\beta = 0.01]$ |

REFERENCES

- AGUR, Z. & MEHR, R. (1997). Modelling *Trypanosoma congolense* parasitaemia patterns during the chronic phase of infection in N'Dama cattle. *Parasite Immunology* **19**, 171–182.
- BARNWELL, J. W., HOWARD, R. J., COON, H. G. & MILLER, L. H. (1983). Splenic requirement for antigenic variation and expression of the variant antigen on the erythrocyte membrane in cloned *Plasmodium knowlesi* malaria. *Infection and Immunity* **40**, 985–994.
- BOELE VAN HENS BROEK, M., PALMER, A., ONYIORAH, E., SCHNEIDER, G., JAFFAR, S., DOLAN, G., MEMMING, H., FRENKEL, J., ENWERE, G., BENNETT, S., KWIATKOWSKI, D. & GREENWOOD, B. (1996). The effect of a monoclonal antibody to tumor necrosis factor on survival from childhood cerebral malaria. *Journal of Infectious Diseases* **174**, 1091–1097.
- BORST, P., BITTER, W., MCCULLOCH, R., VANLEEUWEN, F. & RUDENKO, G. (1995). Antigenic variation in malaria. *Cell* **82**, 1–4.
- BRANNAN, L. R., TURNER, C. M. R. & PHILLIPS, R. S. (1994). Malaria parasites undergo antigenic variation at high rates *in vivo*. *Proceedings of the Royal Society of London, B* **256**, 71–75.
- BROWN, K. N. (1973). Antibody induced variation in malaria parasites. *Nature, London* **242**, 49–50.
- BROWN, K. N. & BROWN, I. N. (1965). Immunity to malaria: antigenic variation in chronic infections of *Plasmodium knowlesi*. *Nature, London* **208**, 1286–1289.
- BULL, P. C., LOWE, B. S., KORTOK, M., MOLYNEUX, C. S., NEWBOLD, C. I. & MARSH, K. (1998). Parasite antigens on the infected red cell surface are targets for naturally acquired immunity to malaria. *Nature, Medicine* **4**, 358–360.
- COLLINS, W. E. & JEFFERY, G. M. (1999). A retrospective examination of sporozoite and trophozoite-induced infections with *Plasmodium falciparum*: development of parasitologic and clinical immunity during primary infection. *American Journal of Tropical Medicine and Hygiene* **61** (Suppl.), S4–S19.
- EARLE, W. C. & PEREZ, M. (1932). Enumeration of parasites in the blood of malarial patients. *Journal of Laboratory and Clinical Medicine* **17**, 1124–1130.
- EYLES, D. E. & YOUNG, M. D. (1951). The duration of untreated or inadequately treated *Plasmodium falciparum* infections in the human host. *The Journal of the National Malaria Society* **10**, 327–336.
- GRAU, G. E., TAYLOR, T. E., MOLYNEUX, M. E., WIRIMA, J. J., VASSALLI, P., HOMMEL, M. & LAMBERT, P.-H. (1989). Tumor necrosis factor and disease severity in children with falciparum malaria. *New England Journal of Medicine* **320**, 1586–1591.
- HOSHEN, M. B., HEINRICH, R., STEIN, W. D. & GINSBURG, H. (2000). Mathematical modelling of the within-host dynamics of *Plasmodium falciparum*. *Parasitology* **121**, 227–235.
- JEFFERY, G. M. & EYLES, D. E. (1954). The duration in the human host of infections with a Panama strain of *Plasmodium falciparum*. *American Journal of Tropical Medicine and Hygiene* **2**, 219–224.
- JEFFERY, G. M., YOUNG, M. D., BURGESS, R. W. & EYLES, D. E. (1959). Early activity in sporozoite-induced *Plasmodium falciparum* infections. *Annals of Tropical Medicine and Parasitology* **53**, 51–58.
- KREMSNER, P. G., WINKLER, S., BRANDTS, C., WILDLING, E., JENNE, L., GRANINGER, W., PRADA, J., BIENZLE, U., JUILLARD, P. & GRAU, G. E. (1995). Prediction of accelerated cure in *Plasmodium falciparum* malaria by the elevated capacity of tumor necrosis factor production. *American Journal of Tropical Medicine and Hygiene* **53**, 532–538.
- KWIATKOWSKI, D. (1995). Malarial toxins and the regulation of parasite density. *Parasitology Today* **11**, 206–212.
- KWIATKOWSKI, D., HILL, A. V. S., SAMBOU, I., TWUMASI, P., CASTRACANE, J., MANOGUE, K. R., CERAMI, A., BREWSTER, D. R. & GREENWOOD, B. M. (1990). TNF concentration in fatal cerebral, non-fatal cerebral, and uncomplicated *Plasmodium falciparum* malaria. *The Lancet* **336**, 1201–1204.
- KWIATKOWSKI, D., MOLYNEUX, M. E., STEPHENS, S., CURTIS, N., KLEIN, N., POINTAIRE, P., SMIT, M., ALLAN, R., BREWSTER, D. R., GRAU, G. E. & GREENWOOD, B. M. (1993). Anti-TNF therapy inhibits fever in cerebral malaria. *Quarterly Journal of Medicine* **86**, 91–98.
- MOLINEAUX, L. (1996). *Plasmodium falciparum* malaria: some epidemiological implications of parasite and host diversity. *Annals of Tropical Medicine and Parasitology* **90**, 379–393.
- MOLINEAUX, L. & DIETZ, K. (1999). Review of intra-host models of malaria. *Parasitologia* **41**, 221–231.
- PHILLIPS, R. S., BRANNAN, L. R., BALMER, P. & NEUVILLE, P. (1997). Antigenic variation during malaria infection – the contribution from the murine parasite *Plasmodium chabaudi*. *Parasite Immunology* **19**, 427–434.
- ROBERTS, D. J., CRAIG, A. G., BERENDT, A. R., PINCHES, R., NASH, G., MARSH, K. & NEWBOLD, C. I. (1992). Rapid switching to multiple antigenic and adhesive phenotypes in malaria. *Nature, London* **357**, 689–692.
- SUTHERLAND, C. J. (1998). The flip-side of cytoadherence: immune selection, antigenic variation and the *var* genes of *Plasmodium falciparum*. *Parasitology Today* **14**, 329–332.